ACTA IMEKO
ISSN: 2221-870X
March 2020, Volume 9, Number 1, 1 - 7

Metrological characterization of instruments for the Body Impedance Analysis

Valerio Marcotuli[1], Matteo Zago[2], Alex P. Moorhead[1], Marco Vespasiani[3], Giacomo Vespasiani[3], Marco Tarabini[1]

[1] *Department of Mechanical Engineering, Politecnico di Milano, via Privata Giuseppe La Masa 1, 20156 Milan, Italy*
[2] *Faculty of Exercise and Sports Science, Università degli Studi di Milano, Via Festa del Perdono 7 - 20122 Milan, Italy*
[3] *Technical Department, Metadieta s.r.l., Via Antonio Bosio, 2, 00161 Rome, Italy*

ABSTRACT
Body impedance analysis (BIA) is used to evaluate the human body composition by measuring the human tissues resistance and reactance with a high-frequency, low-intensity electric current. Nonetheless, the estimation of the body composition is influenced by many factors: body status, environmental conditions, instrumentation, and measurement procedure. This work studies the effect of the connection cables, conductive electrodes, adhesive gel, and BIA device characteristics on the measurement uncertainty. Tests were initially performed on electric circuits with passive elements and on a jelly phantom simulating the body characteristics. The results showed that the cables mainly contribute to increase the error on the resistance measurement, meanwhile the electrodes and the adhesive introduce a negligible disturbance on the measurement chain. This paper also proposes a calibration procedure based on a multivariate linear regression to compensate the systematic error of BIA devices..

Section: RESEARCH PAPER

Keywords: Bioimpedance; body composition; measurement uncertainty; calibration; multivariate linear regression.

Citation: Thomas Bruns, Dirk Röske, Paul P. L. Regtien, Francisco Alegria , Template for an Acta IMEKO paper, Acta IMEKO, vol. A, no. B, article C, Month Year, identifier: IMEKO-ACTA-A (Year)-B-C

Section Editor: name, affiliation

Received month day, year; **In final form** month day, year; **Published** Month Year

Funding:
Corresponding author: Paul P. L. Regtien, e-mail: paul@regtien.net

1. INTRODUCTION

Body composition describes the main components of the human body in terms of free fat mass (FFM), fat mass (FM) or their ratio FFM / FM. The analysis of body composition is used in different fields such as biology and medicine to estimate the nutritional status, muscular volume variations and potentially event pathological status. For example, physiological aging leads to a reduction of FFM and muscular mass, meanwhile fat increases and is redistributed over the body areas [1].

Different levels of body composition, atomic, molecular cellular, tissular and global, can be analyzed depending on the measurement methods [2]. Body mass index (BMI) is a generic indicator of the body composition, but it tends to give inaccurate information when subjects are highly overweight or obese, because it is possible that malnutrition exists yet is masked by the high amount of fat mass [3].

A solution for measuring body composition is represented by the Dual-energy X-ray Absorptiometry (DXA). This is an imaging technique, similar to Magnetic Resonance Imaging (MRI), which scans the patient with two beams of x-rays with different energy (usually 40 and 70kV). In recent years DXA has become recognized as the "gold standard" for measuring body composition [4]. It evaluates both the global and the regional distribution of the three main body components: bone mineral content (BMC), FM and FFM. The accuracy of DXA makes it very effective in studying patient composition within specific body regions and evaluating their effect on the patient health [5]. Unfortunately, a DXA machine is very expensive ($20,000+) making it typically available only to big infrastructure such as clinics and hospitals. An alternative technique is the Bioelectrical Impedance Analysis (BIA) which makes use of a low alternate current (AC) with high frequency at 50 kHz transmitted across the body to estimate its composition based on the hydration level

of tissues [6]. BIA allows for quick examinations, is much less expensive than DXA, and is less dangerous as it does not use of x-rays, meaning it can be also repeated multiple times with no contraindications. Nevertheless, BIA can be highly affected by many factors such as altered hydration of the subject, measurement conditions, ethnic background, and health conditions [7].

BIA devices measure the magnitude of the impedance opposed to the current that varies with respect to the body anatomy. Specifically, the physical principle assumes that the body is comprised of tissues with different composition. Some of which are good conductors due to their water content while others are insulators. The water content is inversely related to the resistance that opposes the current flow. Meanwhile cellular membranes, able to accumulate electrical loads, can be considered capacitors. The presence of capacitors is directly proportional to reactance and introduces an observable delay on the current flow. The sum of the resistance and reactance define the impedance. Its evaluation indicates the body hydration and provides an estimate of the nutritional state equivalent to the cellular amount. Since water is the main component of the cells and it is almost absent in fat, it is possible to deduce the amount of FFM from the water content. Consequently, FM is evaluated by simply subtracting the FFM to the total weight [8].

1.1. Fricke's Circuit: a human body electrical model

The human body consists of resistance and capacitance connected in parallel or in series. The most common body model used in the field of BIA is the *Fricke's circuit*, whose two parallel branches represent the intracellular and extracellular components. In this model, a high frequency current passes through the intracellular water, while at low frequencies through the extracellular space. This is because at zero or low frequency, the current does not penetrate the cell membrane (acting as an insulator), meanwhile it passes through the extracellular medium made of water and sodium [9].

The intracellular behavior, in turn, can be expressed by a resistance R_i due to the water and potassium content and a capacitance X_c of the cell membrane, meanwhile the extracellular behavior is described by a single resistance R_e as in Figure 1. The total body resistance R measured by a BIA instrument is in turn a combination of the two resistances R_i and R_e which indicate the real part of a complex number [10]. Generally, the phasor and other indices such the ratio R_i/R_e can be good estimators of diseases presence, nutritional status, and hydration condition[11].

1.2. The calibration plots

The Cole-Cole plot is a powerful tool to visualize the electrical response of body measurements with the resistance R

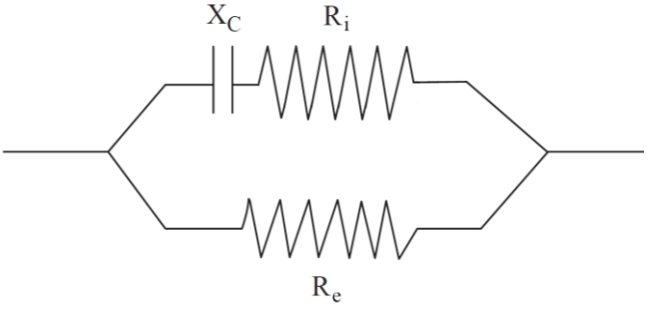

Figure 1. Fricke's circuit model for body composition consisting into two branches related to the intracellular and extracellular behaviors.

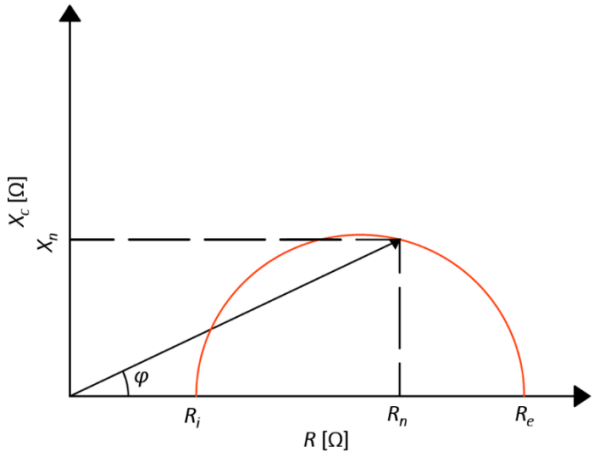

Figure 2. Example of Cole-Cole plot of the Fricke's circuit.

on the x-axis and the negative reactance X_c on the y-axis. At very high or ideally infinite frequency, the intracellular branch is the only one with the minimum resistance value R_i.

At low or zero frequency, the current passes only in the extracellular space since the cell membranes act as insulators. Consequently, the maximum value of resistance is represented by R_e. The relationship between the capacitance X_c and the total resistance R of a body can be expressed by a phase angle φ [12]. Therefore, the resulting phasor ranging from R_i and R_e describes an arc segment as in Figure 2 and all the measured values would lie below it. This plot can be standardized with respect to height, gender, and ethnicity, to form a calibration model divided into adjacent areas contained in tolerance ellipses at 50%, 75%, and 95% belonging to a certain population group (as seen in Figure 3) [13].

The plot is used as a calibration map by companies for converting a measurement performed by means of a device into a body status information [14]. If the BIA device displays a low measurement accuracy, the readings could erroneously suggest the correspondent body status.

1.3. Measurement uncertainty

The biasing factors on bioimpedance estimation can be attributed to the subject (anthropometry, gender, ethnicity, age), to the measurement protocols, and to the instrumentation [15].

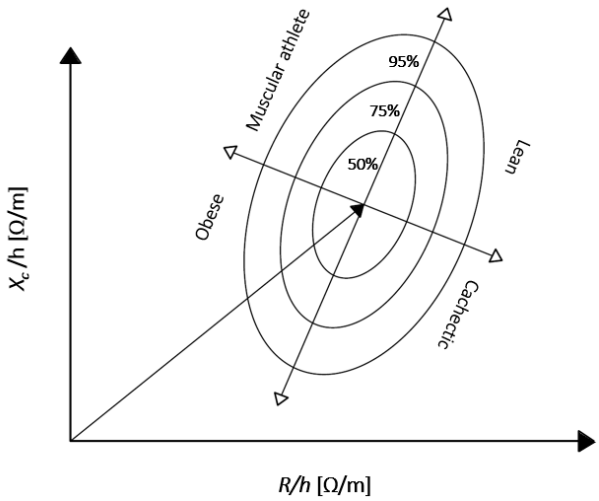

Figure 3. Example of a calibration model standardized by the height (h).

In this study we investigate the possible source of errors of the BIA instrumentation, consisting in a control unit, cables, and electrodes.

The control unit is composed of electronic circuitry placed in a case with one or more ports for connecting the cables. Even if protected, the circuitry is subjected to thermal, electrical, and magnetic disturbances [16,17]. The search for these disturbances is essential for the performances of the devices and to improve competitivity in the market. For this reason, the control unit and the accessories should be metrologically characterized by a specific test for each possible sources of error [18,19]. Moreover, if the disturbances are properly identified, a corrective calibration strategy can be applied [20,21].

2. MATERIALS AND METHODS

2.1. Instrumental equipment

The instrumentation selected for this study consists of *Metadieta Bia*, a BIA device, three sets of cables, three sets of electrodes of different producers, a series of resistances and capacitors, a breadboard.

Metadieta Bia (Figure 4) is an electromedical device for the evaluation of the corporal composition produced by the company Meteda S.r.l. (Rome, Italy). It measures the body impedance response to a sinusoidal current of 350 μA with a single frequency of 50 kHz. The 50 kHz frequency is a *standard de facto* for most BIA devices with a single frequency. The device is a compact (43 x 43 x 12 mm^3) and light weight 50 g making it easily portable due to the lithium battery which can supply the device up to 14 hours in working conditions. It does not have a screen on the control unit, but it can be managed by an application running on phones, tablets, and computers with a Bluetooth connection. The application provides the user the information about the preparation and the execution of the test measurement, then it sends and stores the data on the cloud for later analyses.

The device is designed to be used in clinics by physicians, nutritional biologist, and qualified sanitary personnel but also by consumers in home environments due to its safety and ease of use. Data measurements are then processed on the cloud application and the results can be either quantitative for clinical personnel or qualitative with displayed information in graphs along with the tendences for personal users.

The measurements are performed by placing four electrodes on the hands and feet, with a single cable connected to the main unit.

Figure 4. Metadieta Bia control unit.

The additional equipment for the test is represented by three cables of the same model between the main unit and the 4 electrodes clamps and a series of electrodes of three producers: Biatrodes® by Akern slr (Firenze, Italy), BIA Electrodes by RJL Systems Inc (Clinton Twp, MI, USA), and Regal™ resting ECG by Vermed® Inc (Bells Falls, VT, USA).

2.2. Proposed method

The first operation to perform with a measurement device regards the metrological characterization in terms of repeatability and reproducibility after the identification of the possible sources of error [22]. Generally, this kind of device makes use of empirical equations whose parameters are established by means of a calibration operation performed in laboratory[23]. Since the calibration curves can assume a very large set of values, a simplification of the process can rely on the study of a group of key values.

This research proposes a data selection based on six values of resistance between 200 Ω and 900 Ω with a step of 140 Ω, combined with six values of reactance between 15 Ω and 115 Ω with a step of 20 Ω. These values are represented in the grid in Figure 5.

To assemble a physical circuit starting from the reactance values, suitable capacitors can be identified by converting X_c into a capacitance C with the formula:

$$C = \frac{1}{2 \cdot \pi \cdot f \cdot X_c}, \tag{1}$$

Where the frequency f = 50 kHz of AC emitted by the Metadieta Bia device. The capacitance values obtained after the conversion are therefore: 212 nF, 91 nF, 58 nF, 42 nF, 34 nF, and 28 nF.

By combining the values of resistance and capacitance, we defined a grid of 36 combinations. Since the electrical device consists of different components influencing the reading values, the study of the measurement chain in terms of repeatability and reproducibility is extremely important. Firstly, the components of the chain can be properly selected [23], secondly it is possible to identified two corrections terms R_a and X_a to eliminate the systematic errors affecting the reading values [24].

2.3. Experimental design

The Metadieta Bia is turned on when the cables are inserted in the miniUSB port and the connection is initiated by the application on a master device.

Measurements are typically performed by placing four electrodes on the hands and feet. The electrodes are silver plated for a low resistance and attached to the skin using an adhesive

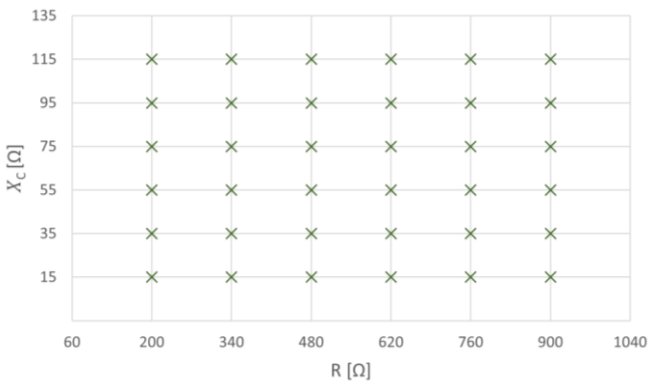

Figure 5. Calibration grid with 36 combinations of the key values selected

Table 1. Resistances and capacitances of the selected components and the reactance values after conversion for the calibration map experiments.

Component	1	2	3	4	5	6
R [Ω]	200	330	470	615	780	910
C [nF]	225	92	51	36	32	27
X_c [Ω]	14	35	56	89	99	120

gel. However, for consistency, all the experiments were performed on laboratory instrumentation with electric circuits representing the body composition through the Fricke's model, consequently the electrodes were included only in specific tests.

The tests were performed in MetroSpace Lab of Politecnico di Milano and can be divided in:

1. Preliminary tests on the metrological characterization of Metadieta Bia device, cables, electrodes, and adhesive gel.
2. Test for systematic error compensation based on the calibration grid in Figure 5.

A high precision LCR meter, model LCR-819 GW Instek (Good Will Instrument Co., Ltd, Taiwan), was used as a reference system for measuring the impedance of the test components, while a multimeter, model Agilent 34401A, was used for the only resistance measurements of the electrical components.

2.4. Preliminary tests

First, the measurement repeatability of the control unit was tested by performing 30 measurements of the resistance R and reactance X_c repeated on 5 different electric circuits connecting the cable clamps directly to the circuit with no other modifications between each test and the next.

The three different cables of the same model have been tested with 30 measurements each with the LCR meter, on the same electric circuit directly connecting the clamps of the cables.

Keeping the same configuration, the effect of the electrodes has been studied applying these components without the adhesive material between the clamps and the electric circuit with passive elements.

We tested 30 different sets of electrodes of the three producers, 4 electrodes for each set. At the same time, the resistance R of the cables and the electrodes was measured 30 times for each component by means of the multimeter device. The measurements on the electrodes were performed by placing the multimeter terminals in two positions, on the tab and on an opposite area far from it (circled in Figure 6).

The effect of the adhesive gel, which determines the interaction with the BIA device and a biological tissue, was simulated by means of a jelly phantom (Figure 7) with nominal resistance of R^{ph}= 571.2 ± 1.2 Ω (C.I. = 68%) and nominal reactance of $X_c{}^{ph}$=75.1±1.9 Ω (C.I. = 68%) [25].

For this test, 30 measurements for each producer's electrode were performed to calculate the mean value of the resistance $\overline{R}$ and reactance $\bar{X}_c$ and the relative standard deviation. The four electrodes were positioned at the borders of the container, one couple on the left side and the other couple on the right side with a distance of about 30 cm. The distance between the two electrodes of each couple was of about 10 cm as recommended by the producer manual.

This configuration with the dominant distance (30 cm > 10 cm) between the two couples of electrodes aimed to replicate the measurement behavior on a human body, avoiding uncontrolled dispersion of the electric charge.

2.5. Tests for systematic error compensation

A set of 36 circuits with passive elements was built by combining selected components with the resistance and capacitance collected in Table 1, to the key values of the calibration grid in Figure 5. Table 1 also includes the reactance values after the conversion obtained by inverting the Eq.1.

The resistances components have a manufacturing tolerance of 0.1% meanwhile the capacitors have a value of 1%. The circuits were mounted on a breadboard and the values read by Metadieta Bia device were compared to the values read by the LCR meter as references [26].

The differences between the measured and the reference allowed to calculate the RMSE and control for the presence of defined patterns related to systematic disturbances. Part of these disturbances was removed by adding two corrections terms R^a and X_c^a, obtained by a least square minimization of a multivariate linear model, to the generic measurements R and X_c in the form:

$$R^{adj} = R + R_a \tag{2}$$

And

$$X_c{}^{adj} = X_c + X_c^a, \tag{3}$$

Where R^{adj} and $X_c{}^{adj}$ are the compensated results.

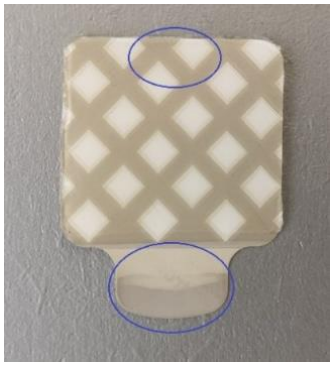

Figure 6. Area of the electrode for measuring the resistance.

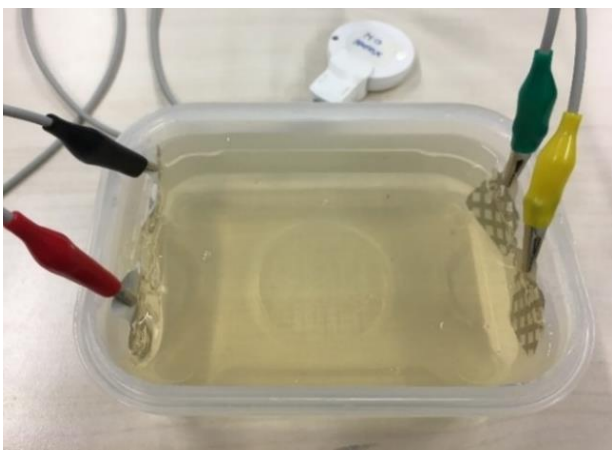

Figure 7. Preliminary test of the electrodes on a jelly phantom.

3. RESULTS

3.1. Preliminary tests

The results of the repeatability test of the control unit on the 5 electric circuits with 30 measurements performed on each circuit are shown in Table 2: R and X_c the key values chosen for the experiments, R^{ref} and X_c^{ref} the reference values read by the LCR meter, $\bar{R}$ and $\bar{X}_c$ the mean values read by the Metadieta Bia device with σ_R and σ_{Xc} the relative standard deviation.

The three tested cables showed a standard deviation of the resistance of σ_R = 1.8 Ω meanwhile the standard deviation of the reactance is σ_{X_c} = 0.1 Ω. From these values it was possible to evaluate the uncertainties as $u_R = \sigma_R/\sqrt{30}$ = 0.33 Ω and $u_{X_c} = \sigma_{X_c}/\sqrt{30}$ = 0.018 Ω (C.I. = 68%).

The electrode without the adhesive gel were tested on a circuit with the nominal resistance of R = 617.812 ± 0.011 Ω (C.I. = 68%) and the equivalent reactance of X_c= 90.137 ± 0.019 Ω (C.I. = 68%) with the Metadieta Bia device. The mean and the standard deviation of the resistance and the reactance are reported in Table 3. The maximum standard deviation values were reported by the RJL systems electrodes equal to σ_R = 0.5 Ω and σ_{X_c} = 0.1 Ω with the correspondent uncertainties of $u_R = \sigma_R/\sqrt{30}$ = 0.091 Ω and $u_{X_c} = \sigma_{X_c}/\sqrt{30}$ = 0.018 Ω (C.I. = 68%).

The resistance-only measurements of the same electrodes performed by means of the multimeter are shown in Table 4. In this case both RJL systems and Vermed® electrodes reported a maximum standard deviation of σ_R = 0.4 Ω and an uncertainty of $u_R = \sigma_R/\sqrt{30}$ = 0.073 Ω (C.I. = 68%).

The last experiment of the preliminary test on the jelly phantom are reported in Table 5. All three electrode samples showed a standard deviation of σ_R = 0.1 Ω with an uncertainty of $u_R = \sigma_R/\sqrt{30}$ = 0.018 Ω (C.I. = 68%), meanwhile Akern and Vermed® electrodes reported a standard deviation different from zero and equal to σ_{X_c} = 0.1 Ω corresponding to an uncertainty of $u_{X_c} = \sigma_{X_c}/\sqrt{30}$ = 0.018 Ω (C.I. = 68%).

3.2. Systematic error compensation

The measurements on 36 electric combinations with the Metadieta Bia device and the reference values are depicted in Figure 8.

From these data, the RMSE of the 36 configurations resulted R_{RMSE} = 4.17 Ω and $X_{c,RMSE}$ = 7.28 Ω. The minimization of the least square on the multivariate linear regression returned the following correction terms:

$$R^a = -1.592 + 0.994 \cdot R + 0.002 \cdot X_c + 2.45 \cdot 10^{-5} \cdot R \cdot X_c \quad (4)$$

And

$$X_c^a = -3.412 + 0.010 \cdot R + 1.079 \cdot X_c - 2.19 \cdot 10^{-5} \cdot R \cdot X_c. \quad (5)$$

With R and X_c the actual values read by the BIA device. Furthermore, the multivariate linear regression reported the adjusted R^2 values of $\bar{R}_R^2$ =0.947 for the resistance and $\bar{R}_{Xc}^2$= 0.696 for the reactance. Compensating for the values in **Error! Reference source not found.** with the terms R^a and X_c^a, the

Table 2. Results of the repeatability test of the control unit on 5 electric circuits.

R[Ω]	X_c [Ω]	R^{ref} [Ω]	X_c^{ref}[Ω]	$\bar{R}$ [Ω]	σ_R[Ω]	$\bar{X}_c$ [Ω]	σ_{Xc}[Ω]
200	15	200.1	17.9	202.7	0	18.9	0.1
200	75	191.4	92.3	193.5	0.1	88.7	0.1
340	115	330.5	124.4	333.4	0.1	116.1	0
620	75	617.8	90.1	622.1	0	80.2	0
900	95	910.9	101.1	916.9	0	98.3	0

Table 3. Results of the repeatability test of the three producer's electrodes without the adhesive gel by means of the Metadieta Bia device.

Producer	$\bar{R}$ [Ω]	σ_R[Ω]	$\bar{X}_c$ [Ω]	σ_{Xc}[Ω]
Akern	619.2	0.2	91.4	0
RJL Systems	619.5	0.5	91.4	0.1
Vermed®	619.4	0.1	91.5	0

Table 4. Results of the repeatability test of the three producer's electrodes without the adhesive gel by means of the multimeter Agilent 34401A.

Producer	$\bar{R}$ [Ω]	σ_R[Ω]
Akern	1.6	0.3
RJL Systems	2.1	0.4
Vermed®	2.1	0.4

Table 5. Results of the repeatability test of the three producer's electrodes with the adhesive gel on the jelly phantom by means of the Metadieta Bia device.

Producer	$\bar{R}$ [Ω]	σ_R[Ω]	$\bar{X}_c$ [Ω]	σ_{Xc}[Ω]
Akern	573.2	0.1	79.1	0.1
RJL Systems	573.3	0.1	78.5	0
Vermed®	573.2	0.1	78.9	0.1

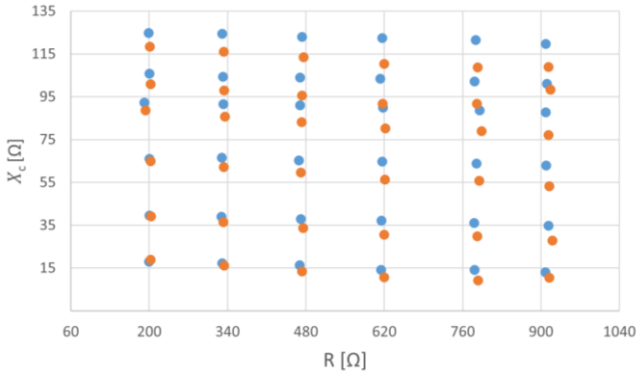

Figure 8. Comparison between the reference values provided by the LCR meter (blue dots) and the measurements performed with the Metadieta Bia device (orange dots).

values of RMSE decrease to R_{RMSE} =1.16 Ω and $X_{c,RMSE}$ =1.28 Ω.

4. DISCUSSION

The tests on the Metadieta Bia device revealed that the cables, the silver-plated electrodes, and the gel have a negligible influence on the overall measurement chain: the cables showed an uncertainty of u_R = 3.3 · 10^{-1} Ω (C.I. = 68%) and u_{X_c}= 1.8 · 10^{-2} Ω (C.I. = 68%) meanwhile the maximum uncertainties introduced by the electrodes were u_R = 8.6 · 10^{-2} Ω (C.I. = 68%) and u_{X_c} = 1.7 · 10^{-2} Ω (C.I. = 68%). The comparison between the three electrode models also showed that these elements have the same electric characteristics for which the device performance does not change as proved by Sanchez et Al. [27]. Also, the tests for the gel on the jelly phantom did not report any significant influence since the maximum uncertainties were u_R = 1.7 · 10^{-2} Ω (C.I. = 68%) and u_{X_c}= 1.7 · 10^{-2} Ω (C.I. = 68%). This means that the adhesive gel is essential for keeping the contact between the electrodes and the skin but it does not add any relevant disturbance to the measurement process [28].

The comparison between the reference values and the measurements with the BIA device in Figure 8 showed that the uncertainties of the reactance and resistance tend to increase for the combinations with higher values. Nonetheless, the trend was corrected effectively by means of the multivariate linear regression. In fact, the two terms R^a and X_c^a can decrease the uncertainties to R_{RMSE} =1.16 Ω and $X_{c,RMSE}$ =1.28 Ω. Moreover, by observing the expressions of R^a, it is evident that the read reactance contribution is negligible. On the contrary, the read resistance value has a relevant influence on the compensation procedure.

5. CONCLUSIONS

BIA is an effective and valid tool to estimate body composition from a fast and safe single measurement. Nonetheless, the estimation can fail when the measurement conditions change or if there is a poor calibration of the BIA device. In this paper we proposed a method to compensate for systematic errors present along the measurement chain of these kind of devices and their equipment. First the equipment was metrologically characterized showing that it does not influence the measurements significantly with uncertainties lower than 0.35 Ω (C.I. = 68%) for both resistance and reactance.

For what concerns the validation of BIA equations, it must be done against gold standards, even though they present limitations due to hydration conditions, age, and ethnicity. This study proposed a calibration grid made of 36 configurations of key values. The grid allowed to calculate multivariate linear models minimizing the least square errors which can be used to calibrate the Metadieta Bia device.

The two correction parameters R_a and X_a obtained from the regression models can reduce the RMSE from 4.2 Ω to 1.2 Ω for the resistance and from 7.3 Ω to 1.3 for the reactance with the adjusted R^2 values respectively of 0.947 and 0.696.
Prospectively, the calibration maps can be extended to higher values and the key points grid can be further populated for more robust results. Eventually, the proposed method can be applied on other BIA devices for comparisons.

REFERENCES

[1] U.G. Kyle, L. Genton, D.O. Slosman, C. Pichard, Fat-free and fat mass percentiles in 5225 healthy subjects aged 15 to 98 years, Nutrition. 17 (2001) 534–541. https://doi.org/10.1016/S0899-9007(01)00555-X.

[2] H.C. Lukaski, Methods for the assessment of human body composition: Traditional and new, Am. J. Clin. Nutr. 46 (1987) 537–556. https://doi.org/10.1093/ajcn/46.4.537.

[3] A. Talluri, R. Liedtke, E.I. Mohamed, C. Maiolo, R. Martinoli, A. De Lorenzo, The application of body cell mass index for studying muscle mass changes in health and disease conditions, Acta Diabetol. 40 (2003). https://doi.org/10.1007/s00592-003-0088-9.

[4] A. Choi, J.Y. Kim, S. Jo, J.H. Jee, S.B. Heymsfield, Y.A. Bhagat, I. Kim, J. Cho, Smartphone-based bioelectrical impedance analysis devices for daily obesity management, Sensors (Switzerland). 15 (2015) 22151–22166. https://doi.org/10.3390/s150922151.

[5] P. Pisani, A. Greco, F. Conversano, M.D. Renna, E. Casciaro, L. Quarta, D. Costanza, M. Muratore, S. Casciaro, A quantitative ultrasound approach to estimate bone fragility: A first comparison with dual X-ray absorptiometry, Meas. J. Int. Meas. Confed. 101 (2017) 243–249. https://doi.org/10.1016/j.measurement.2016.07.033.

[6] M. Dehghan, A.T. Merchant, Is bioelectrical impedance accurate for use in large epidemiological studies?, Nutr. J. 7 (2008) 1–7. https://doi.org/10.1186/1475-2891-7-26.

[7] U.G. Kyle, I. Bosaeus, A.D. De Lorenzo, P. Deurenberg, M. Elia, J.M. Gómez, B.L. Heitmann, L. Kent-Smith, J.C. Melchior, M. Pirlich, H. Scharfetter, A.M.W.J. Schols, C. Pichard, Bioelectrical impedance analysis - Part II: Utilization in clinical practice, Clin. Nutr. 23 (2004) 1430–1453. https://doi.org/10.1016/j.clnu.2004.09.012.

[8] J. Hlubik, P. Hlubik, L. Lhotska, Bioimpedance in medicine: Measuring hydration influence, J. Phys. Conf. Ser. 224 (2010) 012135. https://doi.org/10.1088/1742-6596/224/1/012135.

[9] F. Villa, A. Magnani, M.A. Maggioni, A. Stahn, S. Rampichini, G. Merati, P. Castiglioni, Wearable multi-frequency and multi-segment bioelectrical impedance spectroscopy for unobtrusively tracking body fluid shifts during physical activity in real-field applications: A preliminary study, Sensors (Switzerland). 16 (2016) 1–15. https://doi.org/10.3390/s16050673.

[10] I. V. Krivtsun, I. V. Pentegov, V.N. Sydorets, S. V. Rymar, a Technique for Experimental Data Processing At Modeling the Dispersion of the Biological Tissue Impedance Using the Fricke Equivalent Circuit, Electr. Eng. Electromechanics. 0 (2017) 27–37. https://doi.org/10.20998/2074-272x.2017.5.04.

[11] S. Cigarrán Guldrís, Future uses of vectorial bioimpedance (BIVA) in nephrology, Nefrologia. 31 (2011) 635–643. https://doi.org/10.3265/Nefrologia.pre2011.Oct.11108.

[12] F. Savino, F. Cresi, G. Grasso, R. Oggero, L. Silvestro, The biagram vector: A graphical relation between reactance and phase angle measured by bioelectrical analysis in infants, Ann. Nutr. Metab. 48 (2004) 84–89. https://doi.org/10.1159/000077042.

[13] R. González-Landaeta, O. Casas, R. Pallàs-Areny, Heart rate detection from plantar bioimpedance measurements, IEEE Trans. Biomed. Eng. 55 (2008) 1163–1167. https://doi.org/10.1109/TBME.2007.906516.

[14] F. Ibrahim, M.N. Taib, W.A.B. Wan Abas, C.C. Guan, S. Sulaiman, A novel approach to classify risk in dengue hemorrhagic fever (DHF) using bioelectrical impedance analysis (BIA), IEEE Trans. Instrum. Meas. 54 (2005) 237–244. https://doi.org/10.1109/TIM.2004.840237.

[15] S.F. Khalil, M.S. Mohktar, F. Ibrahim, The theory and fundamentals of bioimpedance analysis in clinical status monitoring and diagnosis of diseases, Sensors (Switzerland). 14 (2014) 10895–10928. https://doi.org/10.3390/s140610895.

[16] A. Ferrero, Measuring electric power quality: Problems and perspectives, Meas. J. Int. Meas. Confed. 41 (2006) 121–129. https://doi.org/10.1016/j.measurement.2006.03.004.

[17] G.M. D'Aucelli, N. Giaquinto, C. Guarnieri Caló Carducci, M. Spadavecchia, A. Trotta, Uncertainty evaluation of the Unified Method for thermo-electric module characterization, Meas. J. Int. Meas. Confed. 131 (2018) 751–763. https://doi.org/10.1016/j.measurement.2018.08.070.

[18] M. Yang, Z. Guan, J. Liu, W. Li, X. Liu, X. Ma, J. Zhang, Research of the instrument and scheme on measuring the interaction among electric energy Metrology of multi-user electric energy meters, Meas. Sensors. 18 (2021) 100067. https://doi.org/10.1016/j.measen.2021.100067.

[19] E. Pittella, E. Piuzzi, E. Rizzuto, S. Pisa, Z. Del Prete, Metrological characterization of a combined bio-impedance plethysmograph and spectrometer, Meas. J. Int. Meas. Confed. 120 (2018) 221–229. https://doi.org/10.1016/j.measurement.2018.02.032.

[20] A. Ferrero, C. Muscas, On the selection of the "best" test waveform for calibrating electrical instruments under nonsinusoidal conditions, IEEE Trans. Instrum. Meas. 49 (2000) 382–387. https://doi.org/10.1109/19.843082.

[21] B. Qi, X. Zhao, C. Li, Methods to reduce errors for DC electric field measurement in oil-pressboard insulation based on Kerr-effect, IEEE Trans. Dielectr. Electr. Insul. 23 (2016) 1675–1682. https://doi.org/10.1109/TDEI.2016.005507.

[22] S. Corbellini, A. Vallan, Arduino-based portable system for bioelectrical impedance measurement, IEEE MeMeA 2014 - IEEE Int. Symp. Med. Meas. Appl. Proc. (2014) 4–8. https://doi.org/10.1109/MeMeA.2014.6860044.

[23] T. Kowalski, G.P. Gibiino, J. Szewiński, P. Barmuta, P. Bartoszek, P.A. Traverso, Design, characterisation, and digital linearisation of an ADC analogue front-end for gamma spectroscopy measurements, Acta IMEKO. 10 (2021) 70–79. https://doi.org/10.21014/acta_imeko.v10i2.1042.

[24] A. Ferrero, M. Lazzaroni, S. Salicone, A calibration procedure for a digital instrument for electric power quality measurement, IEEE Trans. Instrum. Meas. 51 (2002) 716–722. https://doi.org/10.1109/TIM.2002.803293.

[25] M. Peixoto, M.V. Moreno, N. Khider, Conception of a phantom in agar-agar gel with the same bio-impedance properties as human quadriceps, Sensors. 21 (2021). https://doi.org/10.3390/s21155195.

[26] L. Cristaldi, A. Ferrero, S. Salicone, A distributed system for electric power quality measurement, IEEE Trans. Instrum. Meas. 51 (2002) 776–781. https://doi.org/10.1109/TIM.2002.803300.

[27] B. Sanchez, A.L.P. Aroul, E. Bartolome, K. Soundarapandian, R. Bragós, Propagation of measurement errors through body composition equations for body impedance analysis, IEEE Trans. Instrum. Meas. 63 (2014) 1535–1544. https://doi.org/10.1109/TIM.2013.2292272.

[28] T. Ouypornkochagorn, Influence of electrode placement error and contact impedance error to scalp voltage in electrical impedance tomography application, IEECON 2019 - 7th Int. Electr. Eng. Congr. Proc. (2019). https://doi.org/10.1109/iEECON45304.2019.8939016.